



**HAL**  
open science

## Precipitation, soil moisture and runoff variability in a small river catchment (Ardèche, France) during HyMeX Special Observation Period 1

Jessica Huza, Adriaan J. Teuling, Isabelle Braud, Jacopo Grazioli, Lieke A. Melsen, Guillaume Nord, Timothy H. Raupach, Remko Uijlenhoet

► **To cite this version:**

Jessica Huza, Adriaan J. Teuling, Isabelle Braud, Jacopo Grazioli, Lieke A. Melsen, et al.. Precipitation, soil moisture and runoff variability in a small river catchment (Ardèche, France) during HyMeX Special Observation Period 1. *Journal of Hydrology*, 2014, 516, p. 330 - p. 342. 10.1016/j.jhydrol.2014.01.041 . hal-01068013

**HAL Id: hal-01068013**

**<https://hal.science/hal-01068013>**

Submitted on 24 Sep 2014

**HAL** is a multi-disciplinary open access archive for the deposit and dissemination of scientific research documents, whether they are published or not. The documents may come from teaching and research institutions in France or abroad, or from public or private research centers.

L'archive ouverte pluridisciplinaire **HAL**, est destinée au dépôt et à la diffusion de documents scientifiques de niveau recherche, publiés ou non, émanant des établissements d'enseignement et de recherche français ou étrangers, des laboratoires publics ou privés.

Precipitation, soil moisture and runoff  
variability in a small river catchment  
(Ardèche, France) during HyMeX Special  
Observation Period 1

Jessica Huza<sup>(1,2,5)</sup>, Adriaan J. Teuling<sup>(1)</sup>, Isabelle Braud<sup>(2)</sup>,  
Jacopo Grazioli<sup>(4)</sup>, Lieke A. Melsen<sup>(1)</sup>, Guillaume Nord<sup>(3)</sup>,  
Timothy H. Raupach<sup>(4)</sup> Remko Uijlenhoet<sup>(1)</sup>

January 22, 2014

1. Hydrology and Quantitative Water Management Group, Wageningen  
University, Wageningen, The Netherlands
2. UR HHLY, Hydrology-Hydraulics, Irstea, Villeurbanne, France
3. Laboratoire d'étude des Transferts en Hydrologie et Environnement,  
Grenoble, France

4. Environmental Remote Sensing Laboratory, École Polytechnique Fédérale  
de Lausanne, Lausanne, Switzerland
5. Water Department, Environment & Infrastructure, AMEC Americas,  
Montréal, Canada

1 **Abstract**

2 Flash flooding is a potentially destructive natural hazard known  
3 to occur in the Cévennes-Vivarais region in southern France. HyMeX  
4 (Hydrological Cycle in the Mediterranean Experiment) is an interna-  
5 tional program focused on understanding the hydrological cycle in the  
6 Mediterranean basin. Soil moisture is known to be a useful indicator  
7 of catchment response, however, establishing a meaningful estimation  
8 of soil moisture at the catchment level can be difficult due to its high  
9 variability in space and time.

10 In a small gauged catchment in the Cévennes-Vivarais region in  
11 southern France, a series of manual soil moisture measurements was  
12 taken from September to December 2012 at both the field and catch-  
13 ment scale during the Special Observation Period 1 (SOP1) as part  
14 of the HyMeX program. Six plots were selected along a trajectory of  
15 a microwave link installed in the catchment and were chosen to rep-  
16 resent different elevations in the catchment. Within each field plot,  
17 surface soil moisture was measured along a 50 m transect at 2 m in-  
18 tervals. This allowed the study of changes in within-field variability  
19 as well as between-field variability in response to precipitation events  
20 and during the drying out phase.

21 Several precipitation events occurred over this autumn 2012 pe-  
22 riod which caused a significant wetting-up of the catchment, allow-

23 ing the study of soil moisture processes over a wide range of wetness  
24 conditions. The influence of antecedent catchment conditions (soil  
25 moisture) on rainfall-runoff dynamics is demonstrated through the  
26 comparison of storm hydrographs for the various events. Dry catch-  
27 ment conditions result in minimal response in event flow, whereas large  
28 precipitation events occurring during wetter conditions produce much  
29 stronger responses in event flow. This further confirms the importance  
30 of quantifying catchment initial conditions to enhance the prediction  
31 of flash flood occurrences.

32 Keywords: initial soil moisture, small catchments, HyMeX, runoff gener-  
33 ation, temporal stability, soil moisture spatial variability

## 34 **1 Introduction**

35 Orographic precipitation and intense convective systems are common in the  
36 Mediterranean region. They can potentially lead to flash floods, creating  
37 significant environmental and socio-economic impacts. Prediction of these  
38 systems is a challenge due to the complex interaction between oceanic, atmo-  
39 spheric, and hydrological processes (*Ducrocq et al.*, 2010). The Hydrological  
40 cycle in Mediterranean Experiment (HyMeX) is an international initiative  
41 launched in 2007 aiming at a better understanding of the hydrological cycle  
42 and processes in the Mediterranean basin (*Drobinski et al.*, 2013; *Ducrocq*  
43 *et al.*, 2013). One of the focuses includes high impact weather events involv-  
44 ing heavy precipitation and flash flooding.

45 The Mediterranean region is characterized by a hydrological cycle bring-  
46 ing long dry summers where drought often occurs, and wet fall and winter  
47 periods (*Drobinski et al.*, 2013). Typical to this highly variable hydrologi-  
48 cal cycle is the occurrence of heavy precipitation causing flash flooding and  
49 floods (*Gaume et al.*, 2004; *Delrieu et al.*, 2005; *Borga et al.*, 2007; *Gaume*  
50 *et al.*, 2009). The FloodScale project, which is centered around the Cévennes-  
51 Vivarais region in southern France, contributes to the HYMEX initiative and  
52 aims to deepen the understanding of flash flood occurrences and the con-  
53 tributing hydrological processes.

54

55 Soil moisture conditions are of particular importance for predicting hydro-  
56 logical processes because they can influence the relative proportion of rainfall  
57 input among the possible overland and subsurface pathways (*Massari et al.*,  
58 2013). Root zone soil moisture has been shown to influence the dynamics of  
59 evapotranspiration and drainage processes (*Albertson and Kiely*, 2000) lead-  
60 ing to impacts on the partitioning of latent and sensible heat exchanges to  
61 the atmosphere. Furthermore, the antecedent soil moisture conditions of a  
62 catchment have been shown in previous studies to be very influential in pre-  
63 dicting flood occurrence (*De Michele and Salvadori*, 2002; *Norbiato et al.*,  
64 2009; *Sangati et al.*, 2009; *Tramblay et al.*, 2010), also specific for Mediter-  
65 ranean regions (*Massari et al.*, 2013; *Aronica and Candela*, 2004).

66

67 Obtaining representative catchment scale soil moisture measurements,  
68 even in small catchments, can be difficult given the dynamic spatial and  
69 temporal behaviour of soil moisture (*Teuling and Troch*, 2005; *Brocca et al.*,  
70 2009a). Previous studies have shown the influence of topographical features  
71 (*Famiglietti et al.*, 1998; *Brocca et al.*, 2007) and soil properties (*Teuling and*  
72 *Troch*, 2005) on soil moisture values found at the field scale. In a theoretical  
73 study done by *Albertson and Montaldo* (2003), the temporal dynamics of soil  
74 moisture were explored in the context of the relative influences of parameters

75 such as soil, vegetation, precipitation, topography, and initial soil moisture.  
76 All parameters were shown to influence the temporal and spatial dynamics  
77 of soil moisture, proving that obtaining accurate soil moisture conditions at  
78 the catchment scale for use in flood prediction can be difficult.

79

80 Despite soil moisture being highly variable at small scales, soil moisture  
81 fields have been known to display temporal stability. This concept was first  
82 introduced by *Vachaud et al.* (1985) who noticed that, although soil moisture  
83 variability can be quite high, deviations from the spatial mean show a strong  
84 temporal persistence. *Chen* (2006) introduced the term rank stability to de-  
85 scribe the temporal stability of soil moisture. In a review on soil moisture  
86 observation studies, *Vanderlinden et al.* (2012) show that rank stability in  
87 soil moisture has been observed under a wide range of conditions; at different  
88 spatial scales, different temporal scales, and for different soil and vegetation  
89 types, although *Martínez et al.* (2013) showed that a relation exists between  
90 rank stability and climate and soil properties. From this concept, it follows  
91 that a limited number of point measurements might be sufficient to infer  
92 areal or catchment mean values for soil moisture (*Teuling et al.*, 2006; *Brocca*  
93 *et al.*, 2012).

94

95 In addition to in-situ measurements, which are accurate but mainly ap-



96 plicable at smaller scales (*Brocca et al., 2013*), remote sensing data are an  
97 important source to map large scale soil moisture fields. This is achieved  
98 through various widely used satellite products, such as Advanced SCAT-  
99 terometer, ASCAT (*Bartalis et al., 2007*), the Soil Moisture and Ocean Salin-  
100 ity Satellite SMOS (*Kerr, 2007*), Advanced Microwave Scanning Radiometer  
101 for Earth observation, AMSR-E (*Owe et al., 2008*), and the Microwave Imag-  
102 ing Radiometer with Aperture Synthesis, MIRAS (*Kerr et al., 2010*). The  
103 soil moisture data obtained through these sensors are applied in the field of  
104 hydrology for multiple purposes including but not limited to weather anal-  
105 yses and forecasting. Since remote sensing soil moisture products are still  
106 under development (see e.g. *Wagner et al. (2013)*), ground measurements  
107 are of high importance for the validation of remote sensing products (*Cosh*  
108 *et al., 2004*).

109

110 In order to improve the understanding of the rainfall-runoff dynamics of  
111 small Mediterranean catchments, a field measurement campaign was set up  
112 during the HyMeX Special Observation Period (SOP1), which spans from the  
113 period of 14 September 2012 to 5 December 2012. SOP1 is a short period  
114 spanning the seasonal scale where an increased number of hydrological obser-  
115 vations occur in specific catchments. During this period, in situ soil moisture  
116 measurements were conducted in a structured way at various scales. These

117 data have been compared to precipitation data from several sources, and soil  
118 moisture satellite data. This study has the following research objectives; (i)  
119 quantify the temporal and spatial soil moisture variability at the field (or  
120 transect) scale and catchment scale; (ii) determine whether regional-scale  
121 soil moisture measurements can be used for prediction of field-scale hydro-  
122 logical processes; (iii) study the influence of spatio-temporal variability of  
123 precipitation on that of soil moisture; (iv) quantify the relationship between  
124 catchment initial conditions (soil moisture) and runoff processes.

125 First, the research area and the field work strategy will be described, followed  
126 by a presentation of the results obtained through the collection of environ-  
127 mental data. Finally a discussion of the results, along with some perspectives  
128 will be given.

## 129 **2 Data and methods**

### 130 **2.1 Gazel Catchment**

131 The study site is located in the Ardèche catchment, as seen in Figure 1,  
132 which is a mesocale catchment of 2,350 km<sup>2</sup>. In the north eastern part of  
133 this catchment two smaller nested sub-catchments are located; the Claduègne  
134 and the Gazel, which are 43 km<sup>2</sup> and 3.4 km<sup>2</sup> in areas respectively. The field

135 experiments for soil moisture measurements were carried out during the fall  
136 2012 SOP1 in the Gazel, a small sub-catchment of the Ardèche with an area  
137 of 3.4 km<sup>2</sup> (Figure 1). The Gazel catchment is characterized by a steep  
138 south facing slope in the northern part that becomes more gradual near the  
139 southern part of the catchment. The elevation of the upper part of the  
140 catchment is roughly 630 m, while the elevation at the catchment outlet is  
141 approximately 270 m. The upper part of the catchment is characterized by  
142 basalt formations, after which a sharp transition occurs where the lower two  
143 thirds is made up of sedimentary limestone rock. The soil types are heavily  
144 influenced by the geology of the catchment. Volcanic soils and silty-sandy  
145 soils are found in the upper and lower part of the catchment, respectively. In  
146 addition, proportions of clay are also found in the soils (see Table 1), and the  
147 main land use type is pastures and vineyards. Average annual precipitation is  
148 approximately 1030 mm (based on daily rain gauge data operated by Météo-  
149 France located at Le Pradel (Figure 1) in the catchment for the period of  
150 1958-2000).

## 151 **2.2 Precipitation**

152 Precipitation data were received from the following sources: radar data from  
153 the X-band dual polarization weather radar (spatial and temporal resolution

154 of 75 m and 3 minutes, respectively) located approximately 5 km north east of  
155 the Gazel catchment, rain gauges and disdrometers located in the upper and  
156 lower part of the catchment, and a microwave link running in a north-south  
157 direction (Figure 1). The rain gauge and disdrometer data were received  
158 for the whole period that soil moisture measurements were done. For the  
159 rain gauge located in the village of Mirabel (upper part of the catchment),  
160 only data up to 27 October 2012 were available due to technical issues that  
161 persisted until after the field work was completed.

162 Hourly precipitation sums were computed for both the radar and the dis-  
163 drometer data. In addition, each soil moisture measurement was attributed  
164 a precipitation sum, which was calculated by totalling all rainfall occurring  
165 during the interval of the previous and current soil moisture measurement.  
166 For soil moisture measurements occurring on non-consecutive days, a maxi-  
167 mum of three days leading up to the soil moisture measurement was used as  
168 the interval length for accumulating rainfall depth.

169

## 170 **2.3 Soil moisture data**

171 To evaluate the soil moisture spatial and temporal dynamics, a sampling  
172 strategy was designed that allowed for capturing both soil moisture condi-

173 tions at the catchment scale as well as the field-scale with a single handheld  
174 instrument. Point volumetric soil moisture measurements were done using a  
175 portable three-prong (6 cm rod length) ThetaProbe unit (Delta-T Devices  
176 Ltd, Cambridge, UK), which employs the time domain reflectometry (TDR)  
177 technique. The uncertainty in limiting measurements to the top 6 cm were  
178 compared through side-by-side measurements of five transects with an addi-  
179 tional TRIME-PICO 64 TDR-probe (IMKO GmbH, Ettlingen, DE) having  
180 a rod length of 16 cm. In Figure 2, it can be seen that the two sensors  
181 agree quite well based on the small differences between the sensors. The  
182 6 cm ThetaProbe was chosen for the field measurements because of increas-  
183 ing stoniness with depth found in many fields, which complicated the use of  
184 the TDR with longer rod length.

185

186 Fields were selected to appropriately represent the catchment, while still  
187 capturing inter-field variability and the influence of different topographical  
188 features. The criteria in selecting the location of the different fields through-  
189 out the catchment were the following: two fields should be chosen to be in  
190 close proximity of the rain gauge and disdrometers found at the Le Pradel  
191 and Mirabel sites (blue arrows in Figure 1). The fields in between should  
192 be selected in a way that they are aligned with the path of the microwave  
193 link, and be equally spaced between to account for the variation of altitude

194 in the catchment (increasing towards the north). The following factors were  
195 taken into consideration when selecting the fields: ability to measure, ease  
196 of access, and reduced interference (such as ploughing or tilling of the field).  
197 Vineyards were not selected because the soil was dominated by stones, mak-  
198 ing it impossible to sample without breaking the sensor. This resulted in all  
199 selected fields being pastures and grasslands (see Table 1 for a full description  
200 of the fields selected).

201 Within each of the selected six fields, a transect path of 50 m was mea-  
202 sured. The location of the transect within the field was chosen in order to  
203 capture the spatial heterogeneity of the field. If possible, the transect loca-  
204 tion within the field was selected to align with the path of the microwave  
205 link. Along the 50 m transects, a measurement was taken at spatial intervals  
206 of 2 m and all measurements were done at the same location for each of  
207 the measurement days. On each measurement day, all fields were measured  
208 within a few hours to minimize the influence of evaporation and drainage  
209 processes. The strategy was to select measurement days that aligned with  
210 high precipitation events and to capture both pre-event and post-event soil  
211 moisture conditions whenever possible. Between the period of 14 September  
212 2012 to 5 December 2012, 16 measurement days were completed on the six  
213 different transects. This produced approximately 2,500 soil moisture mea-  
214 surements.

215

216 In addition to soil moisture field data, satellite soil moisture data from  
217 the Advanced Scatterometer (ASCAT) on the meteorological operational  
218 (MetOp) platform sensor (*Figa-Saldaña et al.*, 2002) were downloaded from  
219 <http://www.esa-soilmoisture-cci.org>. This data is downloaded using the TU-  
220 Wien algorithm, more information regarding the algorithm can be found in  
221 *Wagner et al.* (1999) and *Naemi et al.* (2009). The coarse spatial (between  
222 25-50 km) and temporal resolution (revisit time of 1 day or less over Eu-  
223 rope) of this data, as well as its high measurement uncertainties make it a  
224 challenge to validate in situ data. The reliability of soil moisture estimates  
225 from remote sensing data remains a challenge that *Brocca et al.* (2011) have  
226 recently addressed. Correlation coefficients with observed soil moisture data  
227 ranging from 0.71 to 0.81, depending on scaling methods, were obtained for  
228 the ASCAT sensor over different regions in Europe. The remote sensing data  
229 were used for the period of 1 September 2012 to 29 November 2012, and was  
230 rescaled as the output provided by the ASCAT sensor is not volumetric soil  
231 moisture  $\theta_v$ .

## 232 2.4 Soil moisture analysis

233 This work includes the study of the temporal and spatial aspects of the vol-  
234 umetric soil moisture field  $\theta(x, t)$  as vol %, where both  $x$  and  $t$  denote the  
235 spatial and temporal components of the observations. The subscript  $i$  is used  
236 to represent a discrete measurement point in space along a transect up to  
237  $n = 26$  measurements, and the subscript  $j$  is used to distinguish between  
238 the different fields being sampled (Transect A through F) up to  $m = 6$  fields  
239 ( $x_{i,j} = \{x_{A,1}, \dots, x_{m,n}\}$ ).

240

241 Each soil moisture measurement day is defined as  $t_d = \{t_1, t_2, \dots, t_k\}$   
242 where  $d$  refers to the measurement day, with the number of total days being  
243 equal to  $k = 16$ . The volumetric soil moisture at a discrete point along a  
244 transect is denoted by  $\theta(x_{i,j}, t_d)$ , and  $\bar{\theta}(x_j, t_d)$  represents the daily transect  
245 mean for a particular field. The daily catchment mean will be denoted as  $\bar{\theta}_d$ .

246

247 For each measurement day  $d$ , the mean for each of the  $m$  fields is com-  
248 puted  $\bar{\theta}(x_j, t_d)$  as well as the daily catchment mean  $\bar{\theta}_d$ :

$$\bar{\theta}(x_j, t_d) = \frac{1}{n} \sum_{i=1}^n \theta(x_{i,j}, t_d), \quad (1)$$

249

$$\bar{\theta}_d = \frac{1}{m} \sum_{j=1}^m \bar{\theta}(x_j, t_d). \quad (2)$$



250 The standard deviation of the soil moisture observations within the transect  
251  $s(\theta(x_j, t_d))$  and the standard deviation of the means among the different  
252 transects  $s(\theta_d)$  is estimated by:

$$s(\theta(x_j, t_d)) = \sqrt{\frac{1}{n-1} \sum_{i=1}^n (\theta(x_{i,j}, t_d) - \bar{\theta}(x_j, t_d))^2}, \quad (3)$$

253

$$s(\theta_d) = \sqrt{\frac{1}{m-1} \sum_{x=1}^m (\bar{\theta}(x_j, t_d) - \bar{\theta}_d)^2}. \quad (4)$$

254 Using these equations, the relationship between mean soil moisture and its  
255 standard deviation can be studied at both the transect scale and the catch-  
256 ment scale.

257

258 The mean soil moisture of a transect at a specific time  $t$  is estimated  
259 through  $n$  discrete observations, and the uncertainty of this estimate will  
260 decrease as the number of observations increases. The uncertainty of the  
261 transect mean can be computed through calculating the standard error of  
262 the mean. The validity of this equation applies to spatially uncorrelated ob-  
263 servations. Additional measurements were performed during this field work  
264 at a scale smaller than 2 m, in which distances ranging from 1 cm up to 2.8 m  
265 were measured. Large spatial variability was observed at scales much smaller  
266 than 2 m, based on a geostatistical analysis of the data. This implies that  
267 the discrete measurements at 2 m intervals along the transect can indeed be

268 assumed to be spatially independent, which further allows for the application  
269 of this equation. The standard error ( $SE$ ) of the transect mean volumetric  
270 soil moisture  $\theta(x_j, t_d)$  in this example is given by:

$$SE = \frac{s(\theta(x_j, t_d))}{\sqrt{n}}. \quad (5)$$

271

272 Furthermore, the different transects measured can be evaluated in terms of  
273 temporal stability. The spatial difference  $\delta_{j,d}$  is defined as the difference  
274 between the soil moisture transect mean  $\bar{\theta}(x_j, t_d)$  and the catchment mean  
275  $\bar{\theta}_d$  such that:

$$\delta_{j,d} = \bar{\theta}(x_j, t_d) - \bar{\theta}_d. \quad (6)$$

276 The temporal mean difference  $\bar{\delta}_j$  for every site is then estimated as:

$$\bar{\delta}_j = \frac{1}{k} \sum_{d=1}^k \delta_{j,d}. \quad (7)$$

277 In order to rank the fields to determine which field is the most stable site in  
278 time, the field with the smallest temporal mean difference will be considered  
279 as the field that on average best represents the catchment mean soil moisture  
280 on a given day. The variability of the temporal mean difference for each field  
281  $s(\delta_j)$  can be computed as:

$$s(\delta_j) = \sqrt{\frac{1}{k-1} \sum_{d=1}^k ((\delta_{j,d}) - \bar{\delta}_j)^2}. \quad (8)$$

## 282 **2.5 Discharge**

283 At the catchment outlet of the Gazel, the water depth is logged every sec-  
284 ond and averaged over two minute intervals. This depth is converted into a  
285 discharge measurement through a stage-discharge relationship. An optimal  
286 stage-discharge relationship is provided through the Baratin tool (*Le Coz*  
287 *et al.*, 2013), and subsequent minimum and maximum stage-discharge curves  
288 are derived as the 5% and 95% statistical distribution based on Monte Carlo  
289 simulations. The difference between the maximum and minimum discharge  
290 is used to estimate the error of the discharge measurement.

291

292 The discharge data was aggregated to hourly averages over the period  
293 of the field work campaign. To investigate the influence of soil moisture  
294 on runoff processes, the hydrograph of selected storm events were analysed.  
295 The baseflow was removed through a baseflow separation technique where  
296 a minimum flow of 5 consecutive days is computed and turning points are  
297 identified. For more details on this technique readers are referred to *Tallak-*  
298 *sen and Van Lanen* (2004). To further analyse the hydrograph and to allow  
299 for comparison between the events, the runoff ratio (RR) was calculated by  
300 dividing the cumulative event discharge by the cumulative precipitation for  
301 a particular event.

302

## 303 **3 Results**

### 304 **3.1 Precipitation**

305 Precipitation was measured with two disdrometers located in the catchment  
306 at a temporal resolution of 30 seconds (blue arrows in Figure 1). An av-  
307 erage of the two disdrometers was used to provide a daily catchment mean  
308 over the observation period (upper panel of Figure 3). Four events of sig-  
309 nificant precipitation occurred throughout the SOP1, in which soil moisture  
310 measurements are clustered around days that coincide with these strong pre-  
311 cipitation events. Throughout the SOP1, approximately 279 mm of rain was  
312 recorded by the two disdrometers located in the catchment, as compared to  
313 333 mm as recorded by the co-located rain gauges. The rainfall estimates  
314 throughout the period for the lower part of the catchment were 288 mm and  
315 333 mm for the disdrometer and rain gauge, respectively. For the upper part  
316 of the catchment, the disdrometer recorded 269 mm over the same period.  
317 Technical problems occurred at the rain gauge located in the upper part of  
318 the catchment, resulting in only the rain gauge located in the lower part of  
319 the catchment recording precipitation beyond 27 October 2012. For daily

320 intensities recorded throughout SOP1 were  $53 \text{ mm day}^{-1}$  and  $57 \text{ mm day}^{-1}$   
321 for the disdrometer and rain gauges respectively, both recorded in the lower  
322 part of the catchment. If the total precipitation sums as recorded by both  
323 the disdrometer and the rain gauges are compared for the four periods where  
324 soil moisture measurements were done (see section 3.3), it can be seen that  
325 the disdrometer consistently records about 22% less precipitation than the  
326 rain gauges. Without having rain gauge data available in the upper part of  
327 the catchment for the full observation period, it is unclear if this difference  
328 is due to spatial variability of precipitation or related to the measurement  
329 technique itself.

330

331 The precipitation characteristics of five events are compared in Table 2.  
332 Looking at the standard deviation  $\text{sd}(P)$  and coefficient of variation  $\text{CV}(P)$   
333 of the hourly precipitation measured in the lower and upper part of the catch-  
334 ment, it can be seen that the variability was significantly higher within the  
335 catchment in the Event #1 as compared to the other events. More details of  
336 this first event can be found in Table 2, where the total precipitation accu-  
337 mulated over the event period was computed for the upper and lower part of  
338 the catchment through the following four techniques (Table 2): Rain gauges,  
339 disdrometers, X-band dual polarization weather radar, and microwave link  
340 (provides a single path-averaged value along the trajectory of the link). Due

341 to the occurrence of hail in the upper part of the catchment, the ice phase  
342 precipitation was removed from the total measured precipitation by the dis-  
343 drometer near Transect E as seen in Table 3. It can be seen that the different  
344 measurement techniques produce a range of precipitation accumulation val-  
345 ues, with the highest recorded by the rain gauges (24 mm) and the lowest  
346 by the radar (17 mm). This highlights the challenge in obtaining accurate  
347 precipitation measurements.

## 348 **3.2 Soil moisture**

### 349 **3.2.1 Temporal evolution during SOP1**

350 A wide range of soil moisture conditions was captured during the SOP1, as  
351 can be seen in the lower panel of Figure 3. Soil moisture measurements are  
352 indicated by the points in the lower panel, the error bars provide information  
353 related to the range seen at the individual transects (recall that the catchment  
354 mean is an average of the six individual transect fields). At the beginning,  
355 very dry conditions are measured with a soil moisture mean of 12.5 vol % first  
356 recorded in mid-September. However, by the end of the observation period  
357 the catchment has become significantly wetter with a catchment mean soil  
358 moisture of 31.9 vol %. A maximum mean soil moisture is seen near the end  
359 of November, after the occurrence of a significant rainfall event, for which

360 the catchment mean of 38.5 vol % was measured.

361

362 The difference among the six transects, as shown by the error bars in the  
363 lower panel of Figure 3, can be seen to be quite small at the beginning of  
364 the observation period when conditions are dry. The size of the error bars  
365 increases along with increasing soil moisture. Details on the soil moisture  
366 values obtained at the transect scale can be found in Table 1.

367

### 368 **3.2.2 Temporal variability: catchment and field scale**

369 Soil moisture shows a large temporal variability during the dry-wet transition  
370 of SOP1, covering a large soil moisture range. Initial values at the end of sum-  
371 mer were close to wilting point, and approached field capacity after repeated  
372 precipitation events (Figure 3). In addition, there was also a large variabil-  
373 ity of the mean soil moisture between the different transects throughout the  
374 SOP. Approximate 95% confidence intervals for the transect means are shown  
375 in Figure 5, calculated as two times the standard error assuming spatially  
376 independent observations (based on the geostatistical analysis described in  
377 section 3.2.3). Overlapping error bars imply that two transect means may  
378 not statistically different. This assumption was further tested with the *post*  
379 *hoc* Tukey Honestly Significant Difference test (interested readers are referred

380 to *Salkind* (2010)). The Tukey HSD test confirmed the results obtained from  
381 comparing the transect means based on overlapping error bars. Visual in-  
382 spection shows that on DOY 267, 270, and 334, the variability between the  
383 different field means is quite low with all transect means having overlap-  
384 ping error bars. This provides an indication of the variability throughout  
385 the catchment as being small on those particular days. Interestingly enough,  
386 a wide range of soil moisture conditions are seen on those days, with this  
387 behaviour occurring in both dry, mid-range, and wet conditions. The length  
388 of the error bars on these days provides insight into the variability within  
389 the transect. The signal is slightly different at this smaller scale. On DOY  
390 267, the error bar length of all transects is quite small, with DOY 270 and  
391 334 displaying longer error bars, indicating more variability within the field.  
392 It can be concluded that by sampling in a randomly selected field only, the  
393 resulting field-scale soil moisture dynamics will not be representative for the  
394 catchment scale mean.

### 395 **3.2.3 Spatial variability: catchment and field scale**

396 The relation between soil moisture variability and mean soil moisture at the  
397 catchment and field scale is shown in Figure 6, where standard deviations  
398 within-field and between-field along with soil moisture conditions are plotted  
399 separately. Both plots are fitted with a linear regression line along with the



400 95% confidence interval lines. A better fit is seen for the between-field vari-  
401 ability than within-field, as reflected by many more points falling outside the  
402 confidence lines in the former than in the latter. However, it should be noted  
403 that given a limited number of fields (6), the between-field variability cannot  
404 be confidently implied through the computation of the standard deviation.  
405 Nonetheless, using standard deviation as a measure of between-field variabil-  
406 ity can still serve to compare between-field variability among the different  
407 measurement days. During dry conditions, both variabilities show a small  
408 standard deviation of approximately 2 vol %. In humid conditions, between-  
409 field variability increases to approximately 3.5 vol % as the soil moisture  
410 mean approaches 40 vol %. Within-field variability can be anywhere from  
411 2.5 vol % to 7 vol %, with a maximum seen in very wet conditions of 8 vol %.

412

413 Although within-field variability exceeded between-field variability, some  
414 evidence was found for the impact of landscape-scale controls on soil mois-  
415 ture variability. To explore the existence of spatial structure at the transect  
416 scale and the influence of topography (see Table 1 for differences in slope  
417 among the transects), two empirical semivariograms (*Goovaerts, 1997*) were  
418 computed for Transects A and F (Figure 7). The first semivariogram was  
419 based on 101 randomly spaced points ranging from 1 cm to 2.8 m (upper  
420 panel of Figure 7), as well as using all measurements collected throughout

421 the observation period at 2 m intervals (lower panel of Figure 7). Note that  
422 Transect A and F represent end-members for slope and elevation in the Gazel  
423 catchment. The standard deviations are plotted as error bars and based on  
424 the approach shown in the upper panel (101 randomly spaced points), Tran-  
425 sect A shows a larger variability. However, when all points at 2 m spacing are  
426 averaged out for Transect A and F, the latter transect shows a significantly  
427 greater variability as evidenced by the longer error bars. Large variability is  
428 seen at small scales as evidenced by the large nugget in both transects. In  
429 the lower panel, a difference among the transects is seen, with evidence of a  
430 sill in Transect F that is not apparent in Transect A.

431

#### 432 **3.2.4 Temporal stability of the transects**

433 In Figure 8, the transects have been sorted based on their mean difference  
434 with respect to the spatial mean  $\bar{\delta}_j$  in order to investigate the temporal or  
435 rank stability of soil moisture in the Gazel catchment. *Teuling et al.* (2006)  
436 showed that on individual dates the site that on average best represents  
437 the catchment has a low probability of being identified. For that reason, to  
438 identify the site that on average best represents the catchment mean, the  
439 average of the spatial means computed for each of the observation days is  
440 taken. Temporal variability, defined as the standard deviation of the spatial

441 mean difference  $s(\bar{\delta}_j)$ , is plotted as error bars. The transect with  $\bar{\delta}_j$  closest to  
442 zero can be termed as the most rank stable site, and is best for representing  
443 the catchment mean.

444

445 Transect D was found to exhibit the highest rank stability. Not only does  
446 this field have the smallest mean difference with respect to the spatial mean,  
447 but the variability of this difference on any day was smallest, making this  
448 transect likely to be selected based on limited sampling.

### 449 **3.2.5 Precipitation-induced spatial variability**

450 To further investigate the occurrence of large differences among the tran-  
451 sect means (Figure 5), including what hydrological processes may have con-  
452 tributed to these differences, the mean soil moisture observations on DOY  
453 267 and 268 (Event #1) are investigated in more detail along with the pre-  
454 cipitation data. On DOY 267 (23<sup>rd</sup> September 2012), Transects A and E had  
455 very similar transect mean soil moisture values (14.8 vol % and 14.2 vol %  
456 respectively). However, the following day a large scatter in the field means  
457 occurred where Transect A increased up to 32 vol % whereas Transect E  
458 increased only up to 23.9 vol %. This implies a difference in volumetric soil  
459 moisture of 8.1 vol % between the fields.

460

461 Looking at the precipitation data, it can be seen that disdrometer, rain  
462 gauge, and radar data (microwave data excluded due to only a single path-  
463 averaged estimate over the link available rather than values at discrete lo-  
464 cations in space) all show higher precipitation occurring near Transect A  
465 rather than Transect E (Table 3). This analysis shows that the large spatial  
466 variability of precipitation was responsible for the creation of variance in the  
467 mean soil moisture among the transects over these two observation days.

468

469 Precipitation intensity is also relevant to analyse as it can influence soil  
470 moisture due to the occurrence of surface runoff from saturation or infiltra-  
471 tion excess processes. The disdrometer recorded a maximum precipitation  
472 accumulation over a ten minute period of 34 mm and 21 mm, near Transect A  
473 and E, respectively. This is consistent with the accumulated rainfall amounts  
474 received in the lower part of the catchment, pointing towards a larger storm  
475 occurring at Le Pradel as compared to Mirabel during this time period.

476

477 If the difference (Diff) in soil moisture between the two days for Transects  
478 A and E is computed, the amount of infiltrated precipitation that is being  
479 measured in the top 6 cm on the day after the event can be inferred. *Brocca*  
480 *et al.* (2013) used soil moisture data to estimate 1 day and 4 day rainfall  
481 observations with satisfactory results at the basin level. In this study, a dif-

482 ference of 17.2 vol % (equals 10 mm of rain) and 9.7 vol % (6 mm of rain)  
483 was computed for the top 6 cm for Transect A and E, respectively. This pre-  
484 liminary analysis shows that the soil moisture measurements in the top soil  
485 only account for approximately half of what was measured as precipitation  
486 depth by the precipitation measurement equipment. This further illustrates  
487 the fast dynamics of the catchment, and the importance of surface runoff and  
488 drainage processes to deeper soil layers in this catchment.

489

### 490 **3.2.6 Comparison between in situ and satellite data**

491 A time series of the satellite data and the in situ observations over the SOP1  
492 can be seen in Figure 4. The ASCAT output was rescaled with the in situ  
493 data through a linear regression using 14 days (Figure 4). A correlation co-  
494 efficient of 0.55 was obtained through this approach. During some periods  
495 throughout the SOP1, there appears to be a small time shift between the two  
496 measurements. The time series is plotted on a daily time scale, however some  
497 days two measurements were performed followed by none the next day. To  
498 avoid gaps in the time series, the second measurement taken in a day was allo-  
499 cated to the following day. This approach could have contributed to the time  
500 shift seen between these two data sets. By removing one measurement point  
501 where the time difference between the in situ and satellite measurement was

502 the greatest, the correlation coefficient of the linear regression increases to  
503 0.74. Despite the time shifts, overall the in situ observations agree well with  
504 the remote sensing data. Approximately two-thirds of the in situ measure-  
505 ments fall within the measurement uncertainty band of the ASCAT sensor.  
506 The spatial resolutions of the satellite and the in situ observations are quite  
507 different, hence it is to be expected that the two measurement types will not  
508 agree very well. In addition, satellite observations are representative for the  
509 top 2-3 cm, whereas the in situ measurements extend to a depth of 6 cm.  
510 Nonetheless, both data sets follow a similar signal, proving that the satellite  
511 data can be useful tool to fill in gaps of missing in situ data. This is in  
512 line with the results of previous studies on ASCAT soil moisture in France  
513 (*Albergel et al.*, 2009). However, it should be noted that replacement of in  
514 situ data by satellite data remains a challenge due to the need to calibrate  
515 satellite data with in situ data.

### 516 **3.3 Runoff response**

517 Five periods where precipitation occurred during SOP1 are shown in Table 2.  
518 Various characteristics are compared for these periods, namely: cumulative  
519 precipitation ( $P$  sum), standard deviation ( $sd(P)$ ) and coefficient of varia-  
520 tion ( $CV(P)$ ) between the hourly precipitation in the upper and lower part

521 of the catchment, cumulative event flow ( $Q_{event\ sum}$ ), runoff ratio ( $RR$ ), an-  
522 tecedent volumetric soil moisture ( $\bar{\theta}_d$ ), post-event volumetric soil moisture  
523 ( $\bar{\theta}_{d+1}$ ), and ASCAT antecedent volumetric soil moisture (ASCAT  $\bar{\theta}_d$ ). The  
524 base flow has been removed to allow comparison among the different periods.  
525 No antecedent or post-event soil moisture are available for Period 5, there-  
526 fore, Figure 9 shows the hydrographs for the four periods where soil moisture  
527 are available.

528

529 The first two events (Event #1 and #2) show minimal catchment re-  
530 sponse, with very low cumulative event flow occurring. In both events, the  
531 soil moisture increased significantly the day after the storm, showing that  
532 the precipitation input served to replenish the soil moisture storage. The  
533 influence of a dry catchment on runoff response is particularly interesting in  
534 Event #1, where a significant amount of precipitation fell on the catchment  
535 (49 mm), yet hardly any event flow was seen (0.17 mm). If the subsequent  
536 events are explored, the catchment displays an entirely different response.  
537 In Event #3 and #4, large precipitation amounts occur, resulting in signif-  
538 icant rises in event flow. Although no in situ soil moisture measurements  
539 were available prior to the last two events, *Massari et al.* (2013) showed that  
540 this can be overcome by using ASCAT satellite data when no in situ soil  
541 moisture measurement is available. By comparing satellite antecedent soil

542 moisture data with post-event soil moisture, a strong rise following precipi-  
543 tation is seen. By looking at the storm hydrograph, a fast response of event  
544 flow to precipitation input during Event #3 and #4 occurred, followed by a  
545 slow recession in the days after the storm. A similar signal is seen with the  
546 soil moisture measurements, in which a gradual decrease occurred after the  
547 precipitation event.

548

549 The antecedent soil moisture conditions appear to have a large influence  
550 on the occurrence of runoff processes in this catchment. This relationship  
551 was further investigated by analysing the runoff ratio for the five precipita-  
552 tion events shown in Table 2. In Figure 10a, the different runoff ratios are  
553 plotted against their corresponding re-scaled initial soil moisture from the  
554 ASCAT satellite sensor. The error bars for the runoff ratios are based on the  
555 error of the discharge as calculated through the difference between the mini-  
556 mum and maximum stage-discharge curves. The error bars for the re-scaled  
557 ASCAT initial soil moisture represent the re-scaled measurement error from  
558 the satellite. A generally increasing trend is seen where small runoff ratios  
559 occur for dry catchment conditions, and large runoff ratios correspond to  
560 wetter conditions. It can also be seen that small events are shown to result  
561 in very low runoff ratios during both dry and wet conditions. A strongly  
562 nonlinear relationship between (soil moisture) storage and runoff behaviour



563 can be hypothesized.

564

565 The event flow rate at the time of soil moisture measurements is also ex-  
566 amined in Figure 10b. The error bars indicate the maximum and minimum  
567 event flow rates (baseflow removed) due to the uncertainty in the stage-  
568 discharge rating curve (derivation described in Section 2.5). The event flow  
569 is shown to be quite variable for different soil moisture measurements, which  
570 indicates that storm size is an important indicator along with catchment ini-  
571 tial conditions. Small precipitation events will not induce a strong response  
572 in event flow even during wet conditions. However, the catchment will re-  
573 spond strongly to large precipitation events during wet and dry conditions.

574

## 575 **4 Discussion**

### 576 **4.1 Methods**

#### 577 **4.1.1 Soil moisture sensor selection**

578 The selection of the soil moisture sensor used in the field determines the  
579 depth and sampling volume of the soil throughout this study. By using the  
580 portable ThetaProbe unit with a rod length of 6 cm, only the top soil was

581 measured. By looking at differences in soil moisture from two consecutive  
582 measurements days in Table 3, it can be seen that approximately 50% of the  
583 precipitation occurring between two measurements days (DOY 267 and 268)  
584 was measured by this sensor in the top 6 cm. Assuming that surface runoff  
585 and drainage processes being important in this catchment, the fact that the  
586 soil moisture sensor manages to capture such a significant amount of the  
587 precipitation further proves the usefulness of the field data for this study.

588

#### 589 **4.1.2 Field and transect selection**

590 The selection of the fields determined the land use type that was measured,  
591 which can influence soil moisture observations. In this study only pastures  
592 and grasslands were chosen due to the large number of stones found in other  
593 land use types which made it impossible to perform field measurements with  
594 the probe. Although all land use types are important for runoff generation,  
595 vineyards were not considered in this study due to measurement difficulties.

596

597 A 50 m transect within the field was selected to capture the spatial het-  
598 erogeneity of the field, and was chosen in a way to account for the influence  
599 of topographical feature and soil properties on soil moisture. Based on previ-  
600 ous studies (*Western et al.*, 1998, 2004), soil moisture spatial patterns were

601 found to have correlation lengths between 30-60 m. This suggests that a  
602 transect of 50 m is likely too small to fully capture spatial variation at the  
603 field scale. Time constraints required that a single transect per field was  
604 measured, as opposed to multiple transects in each field. Therefore, it was  
605 necessary that the transect was chosen to account for spatial heterogeneities  
606 to best represent the field through a single transect. A spacing of 2 m was  
607 used in this study between discrete measurements along the transect. The  
608 influence of this choice was tested by repeating 101 measurements in two  
609 different fields, whereby the distances between discrete measurements were  
610 as small as 1 cm. No spatial structure was seen on a scale smaller than 2 m  
611 and so it was assumed that the choice of a 2 m spatial resolution did not  
612 significantly impact the study.

613

## 614 **4.2 Temporal variability: catchment and field scale**

615 A summary of the transect scale volumetric soil moisture can be found in  
616 Table 1 (initial, final and maximum volumetric soil moisture is shown), in  
617 which the highest soil moisture was measured in Transect F. However, Tran-  
618 sect C was the wettest field measured at the end of the observation period.  
619 This transect has the highest clay content (Table 1), and is the only field in

620 close proximity to a ditch, where the influence of local groundwater on soil  
621 moisture is possible.

622

### 623 **4.3 Spatial variability: catchment and field scale**

624 The between-field and within-field variance was found to be lower at drier  
625 catchment conditions than at wetter conditions (Figure 6), which is contrary  
626 to what was reported in recent studies, where a convex upward relationship  
627 is becoming more prominent (*Famiglietti et al., 2008; Brocca et al., 2010;*  
628 *Rosenbaum et al., 2012; Brocca et al., 2012*). This may be due to the high  
629 infiltrating soils that characterize this catchment. Drainage processes can  
630 contribute to the creation of variance on non-homogeneous soils (*Albertson*  
631 *and Montaldo, 2003*), which is likely the case in this study due to the high  
632 infiltrating soils that would increase the dynamics of this variance creation.

633

634 To test the influence of micro-topographical features on the variability  
635 within the field, two empirical semivariograms were computed for Transects  
636 A and F where small scale variability (measurement distances less than 2 m)  
637 and the variability at the 2 m interval spacing selected for this study were  
638 investigated (Figure 7). A much larger variability is seen in the upper panel

639 where 101 randomly spaced points were measured, as opposed to the lower  
640 panel, where averages of all measurements at 2 m spacings throughout the ob-  
641 servation period was done. Differences in the semivariograms are seen which  
642 may be linked to topography among other factors such as soil properties. In  
643 the lower panel, the existence of a spatial structure at point distances greater  
644 than 30 m is seen in the field characterized by a large slope (Transect F).  
645 Large nuggets are found in both fields, indicating large variability at small  
646 scales. Both findings agree with *Brocca et al.* (2007), who stated difficulty in  
647 identifying a correlation lengths in flat areas.

648

#### 649 **4.4 Temporal stability of the transects**

650 Transect D was shown to be the most rank stable site in the catchment,  
651 suggesting that this field would be the optimal site to sample if the catch-  
652 ment mean was to be approximated based on measurements in a single field.  
653 Transect D is characterized by the average topographical properties of all the  
654 fields (Table 1) in terms of slope, elevation and soil properties. In addition,  
655 this transect is found in the middle part of the catchment suggesting an av-  
656 erage value for upslope drainage area. This is consistent with *Brocca et al.*  
657 (2009b), who found that sites which are most representative are "located in

658 areas reflecting average topography characteristics, in terms of elevation and  
659 slope". This suggests that the best transects for monitoring catchment mean  
660 conditions can be selected a priori based on field characteristics.

661

## 662 **4.5 Precipitation-induced spatial variability**

663 The large local spatial variability of rainfall seen during the event beginning  
664 on 23<sup>rd</sup> September 2012 (Event #1) is an influencing factor on the variabil-  
665 ity of the soil moisture mean between the different fields, as evidenced by  
666 the large difference in soil moisture measured at Transect A (lower) and E  
667 (upper) of the catchment following the event (Table 3). However, this pre-  
668 cipitation event was also shown to be characterized by some hail in the upper  
669 part of the catchment. The ice phase precipitation was removed from the  
670 disdrometer data located in this part of the catchment. The estimate of  
671 amount of hail or duration remains difficult making the rain gauge the refer-  
672 ence for precipitation (liquid water plus melted solid water) during this event.

673

### 674 **4.5.1 Satellite data instead of in situ data**

675 Capturing pre-event soil moisture measurements for short-term observation  
676 can be a challenge, especially if reliance on accurate weather predictions days

677 in advance is required to reach the field site. Long-term options can include  
678 the installation of a fixed sensor beneath the soil surface, however, the instal-  
679 lation process is intrusive and creates non-natural soil conditions enhancing  
680 preferential flow paths. This can lead to inaccurate estimations of catchment  
681 scale soil moisture when point measurements are used for upscaling. For a  
682 short term observation period, such as in this study, in addition to the desire  
683 to measure multiple locations, a portable unit was considered as the optimal  
684 solution.

685

686 The lack of pre-event in situ soil moisture measurements would normally  
687 limit the analysis of antecedent soil moisture and catchment response. Given  
688 the good agreement between the satellite and in situ soil moisture measured  
689 in this study, the gaps in pre-event in situ soil moisture data can be over-  
690 come by using satellite data to infer antecedent catchment scale soil moisture.

691

## 692 **4.6 Catchment response to soil moisture**

693 The effect of antecedent catchment soil moisture conditions on runoff pro-  
694 cesses was found to be significant in this catchment. By exploring the hy-  
695 drographs of four selected events during the observation period (Figure 9), a

696 link between catchment response and wetness conditions could be made. A  
697 comparison between the first two events (Event #1 and #2) and the last two  
698 events (Event #3 and #4) shows strong rises in event flow following precip-  
699 itation occurring only for Event #3 and #4. The runoff ratios for Event #1  
700 and #3 show a difference of two orders of magnitude despite only approx-  
701 imately 20% more precipitation occurring in the latter as compared to the  
702 former event. This relatively small difference in precipitation amount as com-  
703 pared to runoff ratio, suggests that the antecedent soil moisture conditions  
704 strongly influence in the occurrence of storm runoff. In literature, several  
705 studies have shown the relation between antecedent soil moisture and runoff  
706 ratio (among others *Castillo et al.* (2003); *Massari et al.* (2013)), but also  
707 the classical Curve Number method links antecedent soil moisture conditions  
708 with the runoff ratio (*Ponce and Hawkins*, 1996). *Massari et al.* (2013), who  
709 performed a rainfall-runoff modelling study using varying sources of initial  
710 soil moisture data, including satellite, in situ, modelled, and constant input  
711 data, showed poor model performance when a constant initial soil moisture  
712 was used. *Norbiato et al.* (2009) made a link between larger runoff ratios  
713 occurring at higher antecedent soil moisture conditions in catchments char-  
714 acterized by an average sub-surface storage capacity (not an excessively small  
715 or large groundwater storage). Both studies show the importance of accu-  
716 rately estimating the initial soil moisture conditions for flood studies.



717

718 The relationship between catchment initial conditions and runoff ratio  
719 shows an increasing trend with wetness conditions (Figure 10a), where runoff  
720 is likely to occur above approximately 22 vol %. Given that runoff ratio is not  
721 a physical quantity in itself, more information regarding the spatial character-  
722 istics of precipitation during storm events and pre-event in situ soil moisture  
723 observations would be useful to further analyse this hypothesis. In addition,  
724 it is important to note that the upper and lower part of the catchment do not  
725 respond similarly to precipitation input due to differences in geology. This  
726 was reflected in differences in water level observations (not shown).

727

## 728 **5 Conclusion**

729 In this study, an attempt was made to capture spatial and temporal variabil-  
730 ity of soil moisture with structured field measurements, and to compare these  
731 measurements with different data sources (e.g. precipitation from different  
732 sources, and soil moisture products from remote sensing techniques).

733 The spatial variability in soil moisture was seen to increase with wetness  
734 conditions, at both the catchment and transect scale. Within-field variabil-  
735 ity was found to be greater than between-field variability. A variation in

736 the nugget of the empirical semivariograms from the different transects sug-  
737 gested the influence of micro-topographical features and soil properties on  
738 spatial soil moisture variability. Large variability is seen even at very small  
739 distances within the transects, making estimations of a correlation length  
740 difficult. Topographical features (slope) may enhance spatial structure at  
741 distances greater than 30 m within a transect as evidenced by a sill, however,  
742 more measurements should be done to confirm the consistency of this finding.

743

744 Temporal stability in soil moisture conditions has been observed in the in  
745 situ measurements. One particular transect exhibited the largest rank stabil-  
746 ity of all the six fields. This transect can be characterized as displaying aver-  
747 age values for upslope drainage area, elevation, slope and soil properties, as  
748 compared to the other fields in this study. This indicates that if the selection  
749 of a representative site is desired for catchment mean soil moisture estima-  
750 tion, sites displaying average characteristics should be considered. However,  
751 it was also shown that the spatial characteristics of rainfall influence the  
752 spatial variability of soil moisture within the catchment. Differences of soil  
753 moisture between two fields increased from less than 1 vol % to greater than  
754 8 vol % following the occurrence of a highly spatially variable precipitation  
755 event. This highlights the importance of obtaining high spatial-resolution  
756 and reliable rainfall measurements even at the small catchment scale. When

757 a limited number of soil moisture measurements is considered as catchment  
758 representative, the spatial variability of precipitation events should be taken  
759 into account.

760 .

761 Comparison of the in situ soil moisture measurements with the ASCAT  
762 soil moisture product lead to a correlation coefficient of 0.55. In general the  
763 data agreed well and followed a similar signal, even though both techniques  
764 have different spatial resolutions and a different measuring depth (6 cm for  
765 in situ measurements versus 2-3 cm for the satellite product). The results  
766 showed that there is large potential for satellite data to complement in situ  
767 data.

768 Runoff response was shown to be highly dependent on antecedent soil  
769 moisture conditions. Runoff ratios varied by two orders of magnitude with  
770 a difference of precipitation input of less than 20% between two events. The  
771 strong influence of initial soil moisture conditions on runoff generation fur-  
772 ther underlines the importance of antecedent catchment conditions for flood  
773 prediction at the catchment scale. In the absence of in situ soil moisture  
774 data, satellite data can be a good indicator for catchment conditions.

775

## 776 **6 Acknowledgements**

777 The study was conducted under the HyMeX program, sponsored by Grants  
778 MISTRALS/HyMeX, ANR-2011-BS56-027 FLOODSCALE project and  
779 OHMCV. The authors thank the Environmental Remote Sensing Laboratory  
780 (École Polytechnique Fédérale de Lausanne) for operating and providing the  
781 data from the X-band dual polarization weather radar (MXPol), and Météo-  
782 France for providing long term precipitation data. Hpiconet data was pro-  
783 vided by Gilles Molinié (Precis Mecanique 1000 cm<sup>2</sup> rain gauge) and Alexis  
784 Berne (OTT Parsivel disdrometer). The authors also thank Brice Boudevil-  
785 lain for assistance with the Hpiconet data and to Henk Pietersen for the  
786 microwave link data. In addition, the authors acknowledge the EPLEFPA  
787 Olivier de Serres and the municipality of Mirabel for their hospitality and  
788 their assistance in the experiments. AJT acknowledges the financial sup-  
789 port from The Netherlands Organisation for Scientific Research through Veni  
790 Grant 016.111.002.

791

## 792 **References**

793 Albergel, C., C. Ruediger, D. Carrer, J.-C. Calvet, N. Fritz, V. Naemi, Z. Bar-  
794 talis, and S. Hasenauer (2009), An evaluation of ascat surface soil moisture  
795 products with in-situ observations in southwestern france, *Hydrology and*  
796 *Earth System Sciences*, *13*, 115–124.

797 Albertson, J., and G. Kiely (2000), On the structure of soil moisture time  
798 series in the context of land surface models, *J. Hydrol.*, *243*, 101–119.

799 Albertson, J., and N. Montaldo (2003), Temporal dynamics of soil moisture  
800 variability: 1. theoretical basis, *Water Resour. Res.*, *39*(10), 1274.

801 Aronica, G., and A. Candela (2004), A regional methodology for deriving  
802 flood frequency curves (FFC) in partially gauged catchment with uncertain  
803 knowledge of soil moisture conditions, in *The International Environmental*  
804 *Modelling and Software Society Conference, Osnabruck, Germany*.

805 Bartalis, Z., W. Wagner, V. Naemi, S. Hasenauer, K. Scipal, H. Bonekamp,  
806 J. Figa, and C. Anderson (2007), Initial soil moisture retrievals from the  
807 metop-a advanced scatterometer (ASCAT), *Geophys. Res. Lett.*, *34*, 1–5.

808 Borga, M., P. Boscolo, F. Zanon, and M. Sangati (2007), Hydrometeorologi-  
809 cal analysis of the 29 august 2003 flash flood in the Eastern Italian Alps,  
810 *J. Hydrometeorol.*, *8*, 1049–1066.

811 Brocca, L., R. Morbidelli, F. Melone, and T. Moramarco (2007), Soil moisture  
812 spatial variability in experimental areas of central italy, *J. Hydrol.*, *333*,  
813 356–373.

814 Brocca, L., F. Melone, T. Moramarco, and R. Morbidelli (2009a), Soil mois-  
815 ture temporal stability over experimental areas of central italy, *Geoderma*,  
816 *148*(3-4), 364–374.

817 Brocca, L., F. Melone, T. Moramarco, and V. Singh (2009b), Assimilation of  
818 observed soil moisture data in storm rainfall-runoff modeling, *J. Hydraul.*  
819 *Eng.*, *14*(2), 153–165.

820 Brocca, L., F. Melone, T. Moramarco, and R. Morbidelli (2010), Spatial-  
821 temporal variability of soil moisture and its estimation across scales, *Water*  
822 *Resour. Res.*, *46*, 2516.

823 Brocca, L., S. Hasenauer, T. Lacava, F. Melone, T. Moramarco, W. Wag-  
824 ner, W. Dorigo, P. Matgen, J. Martinez-Fernandez, P. Llorens, J. La-  
825 tron, C. Martin, and M. Bittelli (2011), Soil moisture estimation through  
826 ASCAT and AMSR-E sensors: An intercomparison and validation study  
827 across Europe, *Remote Sens. Environ.*, *115*, 3390–3408.

828 Brocca, L., T. Tullo, F. Melone, T. Moramarco, and R. Morbidelli (2012),

829 Catchment scale soil moisture spatial-temporal variability, *J. Hydrol.*, 422-  
830 423, 63–75.

831 Brocca, L., T. Moramarco, and W. Wagner (2013), A new method for rain-  
832 fall estimation through soil moisture observations, *Geophysical Research*  
833 *Letters*, 40, 853–858.

834 Castillo, V., A. Gómez-Plaza, and M. Martínez-Mena (2003), The role of  
835 antecedent soil water content in the runoff response of semiarid catchments:  
836 a simulation approach, *J. Hydrol.*, 284(1-4), 114–130.

837 Chen, Y.-J. (2006), Letter to the editor on "rank stability or temporal sta-  
838 bility", *Soil Sci. Soc. Am. J.*, 70(1), 306–306.

839 Cosh, M., T. Jackson, R. Bindlish, and J. Prueger (2004), Watershed scale  
840 temporal and spatial stability of soil moisture and its role in validating  
841 satellite estimates, *Remote Sens. Environ.*, 92, 427–435.

842 De Michele, C., and G. Salvadori (2002), On the derived flood frequency  
843 distribution: analytical formulation and the influence of antecedent soil  
844 moisture condition, *J. Hydrol.*, 262, 245–258.

845 Delrieu, G., V. Ducrocq, E. Gaume, J. Nicol, O. Payrastre, E. Yates, P.-E.  
846 Kirstetter, H. Andrieu, P.-A. Ayral, C. Bouvier, J.-D. Creutin, M. Livet,  
847 S. Anquetin, M. Lang, L. Neppel, C. Obled, J. P. du Châtelet, G.-M.



848 Saulnier, A. Walpersdorf, and W. Wobrock (2005), The catastrophic flash-  
849 flood event of 8-9 september 2002 in the Gard region, France: A first  
850 case study for the Cévennes-Vivarais Mediterranean hydrometeorological  
851 observatory, *J. Hydrometeorol.*, 6, 34–52.

852 Drobinski, A., V. Ducrocq, P. Alpert, P. Anagnostou, K. Béranger,  
853 M. Borga, I. Braud, A. Chanzy, S. Davolio, G. Delrieu, C. Estournel,  
854 N. F. Boubrahmi, J. Font, V. Grubisic, S. Gualdi, B. Ivenean-Picek,  
855 C. Kottmeier, V. Kotroni, K. Lagouvardos, P. Lionello, M. C. Llasat,  
856 W. Ludwig, C. Lutoff, A. Mariotti, E. Richard, R. Romero, R. Rotunno,  
857 O. Roussot, I. Ruin, V. H. Santaner, S. Somot, I. Taupier-Letage, J. Tin-  
858 tore, R. Uijlenhoet, and H. Wernli (2013), HyMeX, a 10-year multidisci-  
859 plinary program on the Mediterranean water cycle, *b. Am. Meteorol. Soc.*,  
860 submitted.

861 Ducrocq, V., O. Roussot, K. Béranger, I. Braud, A. Chanzy, G. Delrieu,  
862 P. Drobinski, C. Estournel, B. Ivenean-Picek, S. Josey, K. Lagouvardos,  
863 P. Lionello, M. C. Llasat, W. Ludwig, C. Lutoff, A. Mariotti, A. Montanari,  
864 E. Richard, R. Romero, I. Ruin, and S. Somot (2010), HyMeX science plan,  
865 *Tech. Rep. 2.3.2*, Météo-France.

866 Ducrocq, V., I. Braud, S. Davolio, R. Ferretti, C. Flamant, A. Jansa,  
867 N. Kalthoff, E. Richard, I. Taupier-Letage, P.-A. Ayrat, S. Belamari,

- 868 A. Berne, M. Borga, B. Boudevillain, O. Bock, J.-L. Boichard, M.-N.  
869 Bouin, O. Bousquet, C. Bouvier, J. Chiggiato, D. Cimini, U. Corsmeier,  
870 L. Coppola, P. Cocquerez, E. Defier, J. Delanoë, P. Di Girolamo, A. Doeren-  
871 becher, P. Drobinski, Y. Dufournet, N. Fourrié, J. J. Gourley, L. Labatut,  
872 D. Lambert, J. Le Coz, F. S. Marzano, G. Molinié, A. Montani, G. Nord,  
873 M. Nuret, K. Ramage, B. Rison, O. Roussot, F. Said, A. Schwarzenboeck,  
874 P. Testor, J. Van Balen, B. Vincendon, M. Aran, and J. Tamayo (2013),  
875 HyMeX-SOP1, the field campaign dedicated to heavy precipitation and  
876 flash flooding in the northwestern Mediterranean, *American Meteorologi-  
877 cal Society*, doi:10.1175/BAMS-D-12-00244.1, in press.
- 878 Famiglietti, J. S., J. W. Rudnicki, and M. Rodell (1998), Variability in soil  
879 moisture content along a hillslope transect: Rattlesnake hill, Texas, *J.  
880 Hydrol.*, *210*, 259–281.
- 881 Famiglietti, J. S., D. Ryu, A. A. Berg, M. Rodell, and T. J. Jackson (2008),  
882 Field observations of soil moisture variability across scales, *Water Resour.  
883 Res.*, *44*, 1423.
- 884 Figa-Saldaña, J., J. J. W. Wilson, E. Attema, R. Gelsthorpe, M. R. Drinkwa-  
885 ter, and A. Stoffelen (2002), The advanced scatterometer (ASCAT) on the  
886 meteorological operational (MetOp) platform: A follow on European wind  
887 scatterometers, *Can. J. Remote Sens.*, *28*, 404–412.

888 Gaume, E., M. Livet, M. Desbordes, and J.-P. Villeneuve (2004), Hydrolog-  
889 ical analysis of the river Aude, France, flash flood on 12 and 13 november  
890 1999, *J. Hydrol.*, *286*, 135–154.

891 Gaume, E., V. Bain, P. Bernardara, O. Newinger, M. Barbuc, A. Bateman,  
892 L. Blakškovičová, G. Blöschl, M. Borga, A. Dumitrescu, I. Daliakopoulos,  
893 J. Garcia, A. Irimescu, S. Kohnova, A. Koutroulis, L. Marchi, S. Matreata,  
894 V. Medina, E. Preciso, D. Sempere-Torres, G. Stancalie, J. Szolgay, I. Tsa-  
895 nis, D. Velasco, and A. Viglione (2009), A compilation of data on European  
896 flash floods, *J. Hydrol.*, *367*, 70–78.

897 Goovaerts, P. (1997), *Geostatistics for Natural Resources Evaluation*, no. xiv  
898 + 483 pp in Applied Geostistics Series, Oxford University Press.

899 Kerr, Y. (2007), Soil moisture from space: Where are we?, *Hydrogeol. J.*,  
900 *15*(1), 117–120.

901 Kerr, Y., P. Waldteufel, J.-P. Wigneron, S. Delwart, F. Cabot, J. Boutin, M.-  
902 J. Escorihuela, J. Font, N. Reul, C. Gruhier, S. Enache Juglea, M. Drinkwa-  
903 ter, A. Hahne, M. Martin-Neira, and S. Mecklenburg (2010), The SMOS  
904 mission: New tool for monitoring key elements of the global water cycle,  
905 *P IEEE*, *98*, 666–687.

906 Le Coz, J., B. Renard, L. Bonnifait, F. Branger, and R. Le Boursicaud (2013),

- 907 Combining hydraulic knowledge and uncertain gaugings in the estimation  
908 of hydrometric rating curves: a Bayesian approach, *J. Hydrol.*, *509*, 573–  
909 587, doi:<http://dx.doi.org/10.1016/j.jhydrol.2013.11016>.
- 910 Martínez, G., Y. Pachepsky, and H. Vereecken (2013), Temporal stability of  
911 soil water content as affected by climate and soil hydraulic properties: A  
912 simulation study, *Hydrol. Process.*, *Published online*, doi:10.1002/hyp.9737.
- 913 Massari, C., L. Brocca, S. Barbetta, C. Papathanasiou, M. Mimikou, and  
914 T. Mor (2013), Using globally available soil moisture indicators for flood  
915 modelling in Mediterranean catchments, *Hyrol. Earth Sys. Sci. Discuss.*,  
916 *10*, 10,997–11,033.
- 917 Naemi, V., K. Scipal, Z. Bartalis, S. Hasenauer, and W. Wagner (2009), An  
918 improved soil moisture retrieval algorithm for ers and metop scatterome-  
919 ter observations, *IEEE Transactions on Geoscience and Remote Sensing*,  
920 *47(7)*, 1999–2013.
- 921 Norbiato, D., M. Borga, R. Merz, G. Blöschl, and A. Carton (2009), Controls  
922 on event runoff coefficients in the eastern Italian Alps, *J. Hydrol.*, *375*,  
923 312–325.
- 924 Owe, M., R. de Jeu, and T. Holmes (2008), Multisensor historical climatology

925 of satellite-derived global land surface moisture, *J. Geophys. Res.*, *113*, 1–  
926 17.

927 Ponce, V., and R. Hawkins (1996), Runoff curve number: Has it reached  
928 maturity?, *J. Hydrol. Eng.*, *1*(1), 11–19.

929 Rosenbaum, U., H. R. Bogaen, M. Herbst, J. A. Huisman, T. J. Peterson,  
930 A. Weuthen, A. W. Western, and H. Vereecken (2012), Seasonal and event  
931 dynamics of soil moisture patterns at the small catchment scale, *Water*  
932 *Resour. Res.*, *48*, W10544.

933 Salkind, N. J. (2010), *Encyclopedia of Research Design*, SAGE Publications,  
934 Inc.

935 Sangati, M., M. Borga, D. Rabuffetti, and R. Bechini (2009), Influence of  
936 rainfall and soil properties spatial aggregation on extreme flood response  
937 modelling: An evaluation based on the Sesia river basin, North Western  
938 Italy, *Adv. Water Resour.*, *32*, 1090–1106.

939 Tallaksen, L. M., and H. A. Van Lanen (2004), *Hydrological Drought Pro-*  
940 *cesses and Estimation Methods for Streamflow and Groundwater*, Devel-  
941 opments in Water Science, Elsevier.

942 Teuling, A., R. Uijlenhoet, F. Hupet, E. Van Loon, and P. Troch (2006), Esti-

943 mating spatial mean root-zone soil moisture from point-scale observations,  
944 *Hydrol. Earth Syst. Sci.*, 10, 755–767.

945 Teuling, A. J., and P. A. Troch (2005), Improved understanding of soil  
946 moisture variability dynamics, *Geophys. Res. Lett.*, 32(5)(5), L05404, doi:  
947 10.1029/2004GL021935.

948 Tramblay, Y., C. Bouvier, C. Martin, J.-F. Didon-Lescot, D. Todorovik, and  
949 J.-M. Domergue (2010), Assessment of initial soil moisture conditions for  
950 event-based rainfall-runoff modelling, *J. Hydrol.*, 387, 176–187.

951 Vachaud, G., A. Passerat de Silans, P. Balabanis, and M. Vauclin (1985),  
952 Temporal stability of spatially measured soil water probability density  
953 function, *Soil Sci. Soc. Am. J.*, 49, 822–828.

954 Vanderlinden, K., H. Vereecken, H. Hardelauf, M. Herbst, G. Martinez,  
955 M. Cosh, and Y. Pachepsky (2012), Temporal stability of soil water con-  
956 tents: A review of data and analyses, *Vadose Zone J.*, 11(4).

957 Wagner, W., G. Lemoine, and H. Rott (1999), A method for estimating  
958 soil moisture from ers scatterometer and soil data, *Remote Sensing of the*  
959 *Environment*, 70(2), 191–207.

960 Wagner, W., J. Figa, C. Albergel, L. Brocca, S. Hahn, S. Hasenauer, and  
961 W. Dorigo (2013), *Operations, challenges and prospects of satellite-based*

962 *surface soil moisture monitoring services. In: Remote Sensing of Energy*

963 *Fluxes and Soil Moisture Content*, CRC Press.

964 Western, A. W., G. Blöschl, and R. B. Grayson (1998), Geostatistical char-

965 acterisation of soil moisture patterns in the Tarrawarra catchment, *J. Hy-*

966 *drol.*, 205, 20–37.

967 Western, A. W., S.-L. Zhou, R. B. Grayson, T. A. McMahon, G. Blöschl, and

968 D. J. Wilson (2004), Spatial correlation of soil moisture in small catchments

969 and its relationship to dominant spatial hydrological processes, *J. Hydrol.*,

970 286, 113–134.

Table 1: Summary of the transect mean in situ volumetric soil moisture (vol %) over the fall 2012 SOP, along with limited topographical and soil properties, as well as land use for each of the transects measured. Initial, final and maximum mean in situ volumetric soil moisture is shown for each of the transects as Initial  $\theta_v$ , Final  $\theta_v$  and Max  $\theta_v$ , respectively.

Transect	Slope (-)	Porosity (-)	% Sand	% Silt	% Clay	Initial $\theta_v$	Final $\theta_v$	Max $\theta_v$	Land Use
A	0.006	0.55	43	12	45	12.57	30.68	36.69	pasture
B	0.133	0.53	47	18	36	13.50	27.59	36.13	pasture
C	0.059	0.66	35	19	46	16.09	35.34	38.64	grassland
D	0.120	0.59	44	20	36	14.68	33.63	36.52	grassland
E	0.130	0.59	42	16	42	14.23	32.42	42.74	grassland
F	0.230	0.62	46	17	38	14.51	31.47	43.22	grassland



Table 2: Comparison of five precipitation events during the fall 2012 SOP.  $P$  Sum represents the total accumulated hourly precipitation as measured by the disdrometers over the event period. Standard deviation and coefficient of variation, denoted by  $sd(P)$  and  $CV(P)$ , of the precipitation data measured at the Le Pradel and Mirabel locations.  $Q_{event}$  Sum represents the flow discharged over the event period, with pre-event discharge denoted as  $Q_i$ . The runoff ratio (RR) is calculated by dividing  $Q_{event}$  Sum by  $P$  Sum. The volumetric soil moisture prior to the precipitation event for in situ and satellite sources are represented by  $\theta_i$  and ASCAT  $\theta_i$ , respectively. The post-event in situ volumetric soil moisture data is denoted by  $\theta_{i+1}$ . Dates include: 23-28 September (Event #1), 19-22 October (Event #2), 9-17 November (Event #3), 22 November-1 December (Event #4), and 23-31 October (Event #5).

Characteristic	Units	Event #1	Event #2	Event #3	Event #4	Event #5
$P$ Sum	mm	49	8	63	45	47
$sd(P)$	mm	0.04	0.002	0.002	0.005	0.006
$CV(P)$	-	0.13	0.03	0.005	0.02	0.02
$Q_{event}$ Sum	mm	0.17	0.0079	21.17	18.85	0.39
$Q_i$	$l s^{-1}$	0.44	0.78	14.3	13.1	0.97
RR	-	0.0035	0.0012	0.29	0.38	0.011
$\theta_i$	vol %	14	23	-	-	-
$\theta_{i+1}$	vol %	27	31	34	39	-
ASCAT $\theta_i$	vol %	16	23	22	24	27

Table 3: Influence of spatial variability of precipitation on volumetric soil moisture variability among Transect A and E during Event #1. Hourly accumulated precipitation amounts from the rain gauge (Gauge), disdrometer (DSD), radar (Radar) and microwave link (Link) are shown. *P* calc denotes the precipitation estimate using the differences of in situ soil moisture measurements from the 23<sup>rd</sup> (2309) and 24<sup>th</sup> (2409) September 2012 over the top 6 cm.

Transect	Soil Moisture (vol %)				Precipitation (mm)				Max Int (mm 10 min <sup>-1</sup> )
	2309	2409	Diff	<i>P</i> calc	DSD	Gauge	Radar	Link	P int
A	14.8	32.0	17.2	10	24	30	23	-	34
E	14.2	23.9	9.7	6	15	18	11	-	21
Catchment					20	24	17	19	

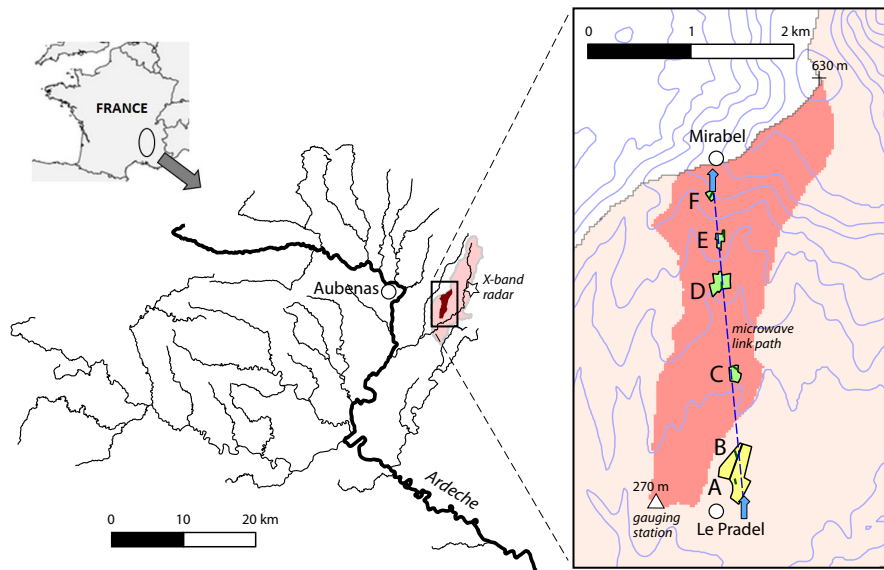


Figure 1: Map of the Ardèche catchment and the Gazel sub-catchment, including measurements being done over the fall 2012 SOP1 in the Gazel catchment. Blue arrows indicate the locations of the disdrometer, rain gauges, as well as the transmitting and receiving ends of the microwave link. Circles represent the villages of Mirabel and Le Pradel. Letters show the locations of the 50 m transects measured throughout the SOP1, which are found in line with the microwave link path (dotted line). The rain gauge operated by Météo-France is located within 200 m of the lower blue arrow at Le Pradel.

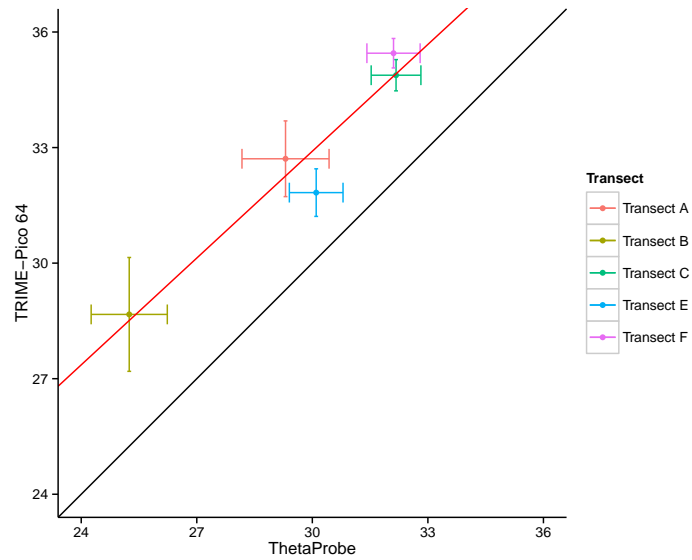


Figure 2: Comparison of volumetric soil moisture transect means on the 14<sup>th</sup> November 2012 with the ThetaProbe (rod length 6 cm) and TRIME-Pico 64 (rod length 16 cm). Error bar lengths based on the standard error  $SE$  of the transect means.

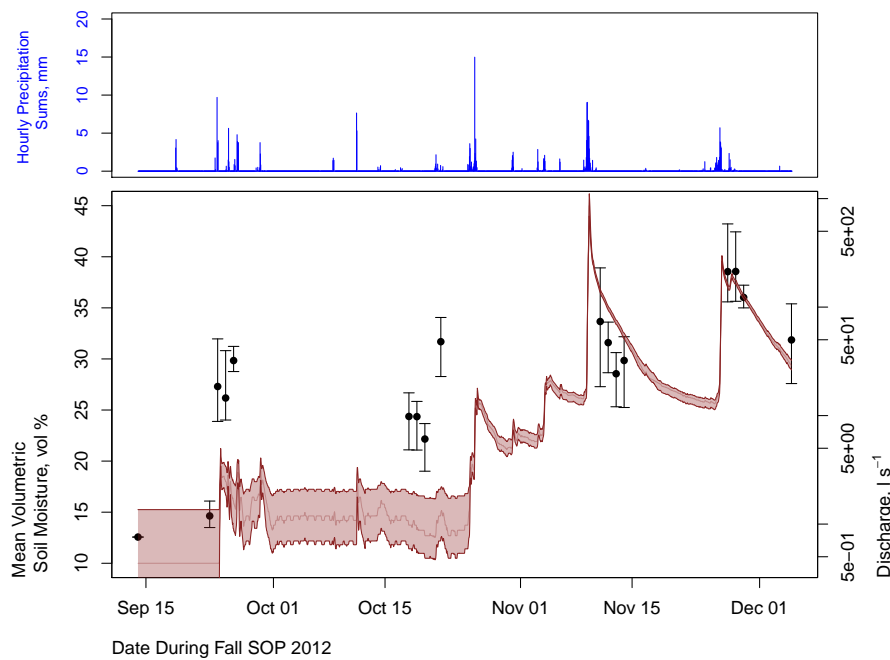


Figure 3: Upper panel: Hourly accumulations for precipitation in mm as estimated by averaging the two disdrometers located in the upper and lower part of the catchment. Lower panel: Mean volumetric in situ soil moisture (vol %) at the catchment scale throughout the SOP. The brown curve shows the discharge in  $l s^{-1}$ , with catchment mean volumetric in situ soil moisture measurements (black dots) along with  $\pm$  standard deviation as error bars. Four precipitation events are seen on the following dates: 23-28 September (Event #1), 19-22 October (Event #2), 9-17 November (Event #3), and 22 November-1 December (Event #4).

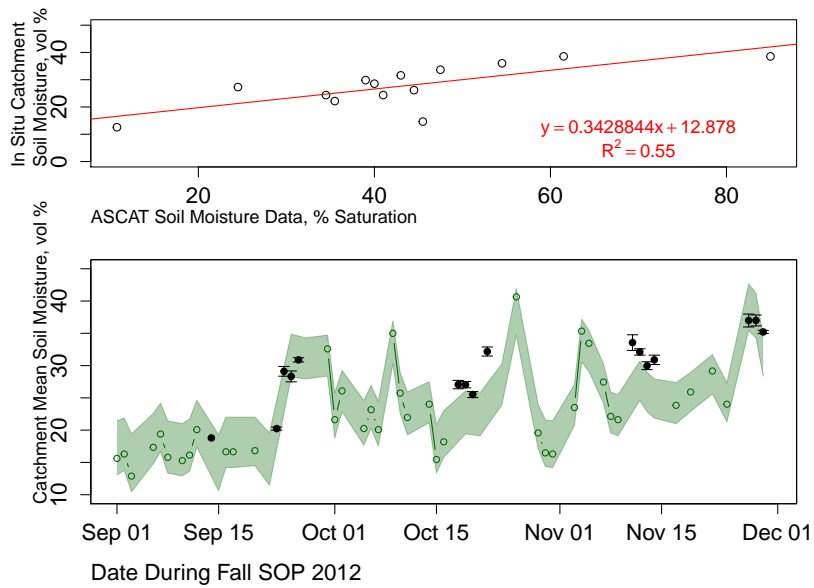


Figure 4: Upper panel: Linear regression of ASCAT satellite observations with in situ volumetric soil moisture measurements (daily catchment means). Lower panel: Time series of ASCAT volumetric soil moisture (open circles) as derived by a linear regression with in situ catchment mean measurements. The error bands (green band) represent the measurement error for the re-scaled ASCAT (*Figa-Saldaña et al., 2002*) data. Catchment mean in situ volumetric soil moisture measurements (filled circles) with error bars based on  $\pm$  the standard deviation are also shown.

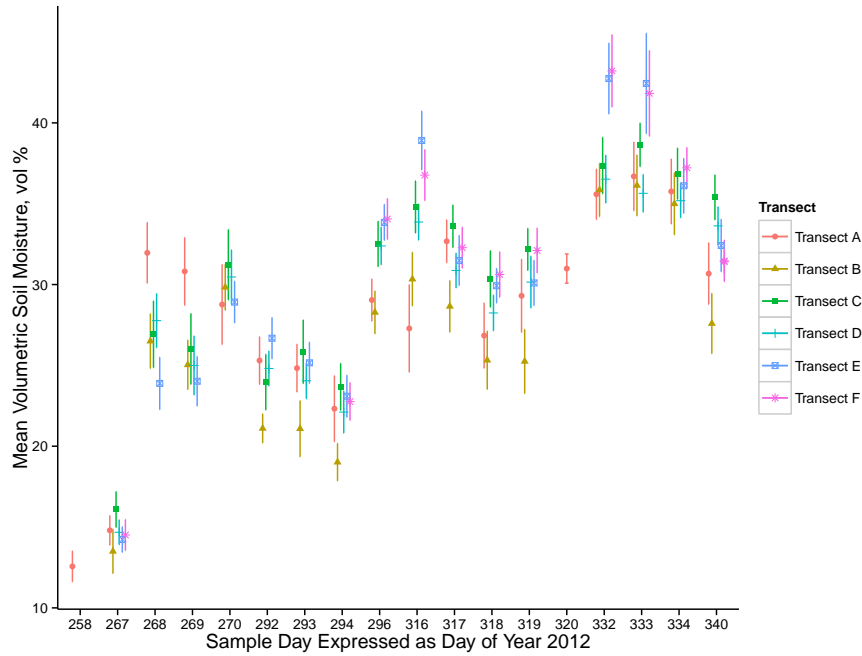


Figure 5: Transect mean volumetric in situ soil moisture for all measurement days as represented by Day of Year (DOY). Error bars indicate 2 times  $\pm SE$ .

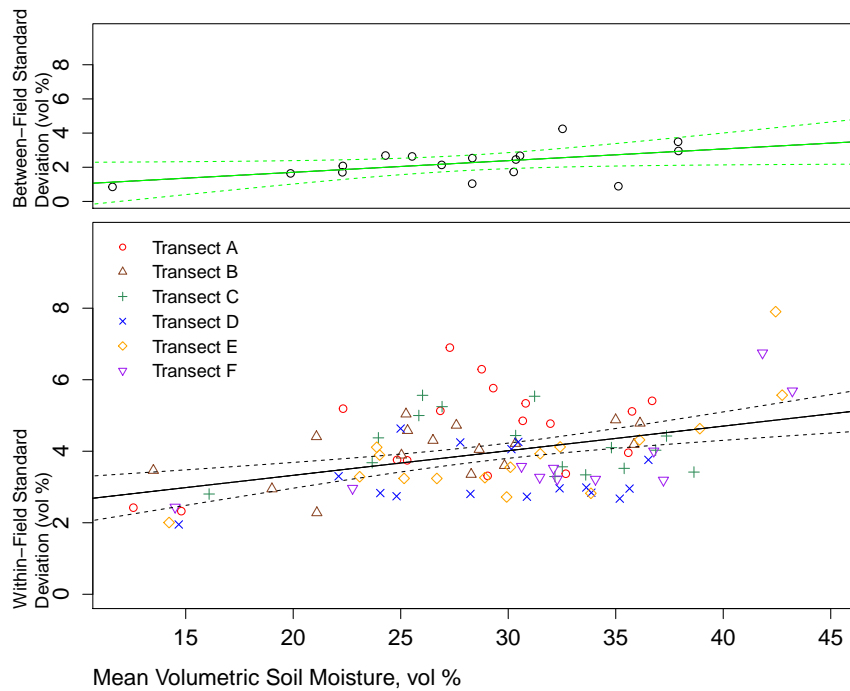


Figure 6: Relationship between mean volumetric in situ soil moisture (vol %) and standard deviation at varying soil moisture conditions. Dotted lines represent a linear fit of the data and solid lines denote the 95% confidence intervals. Upper panel: within-field variability. Lower panel: between-field variability.



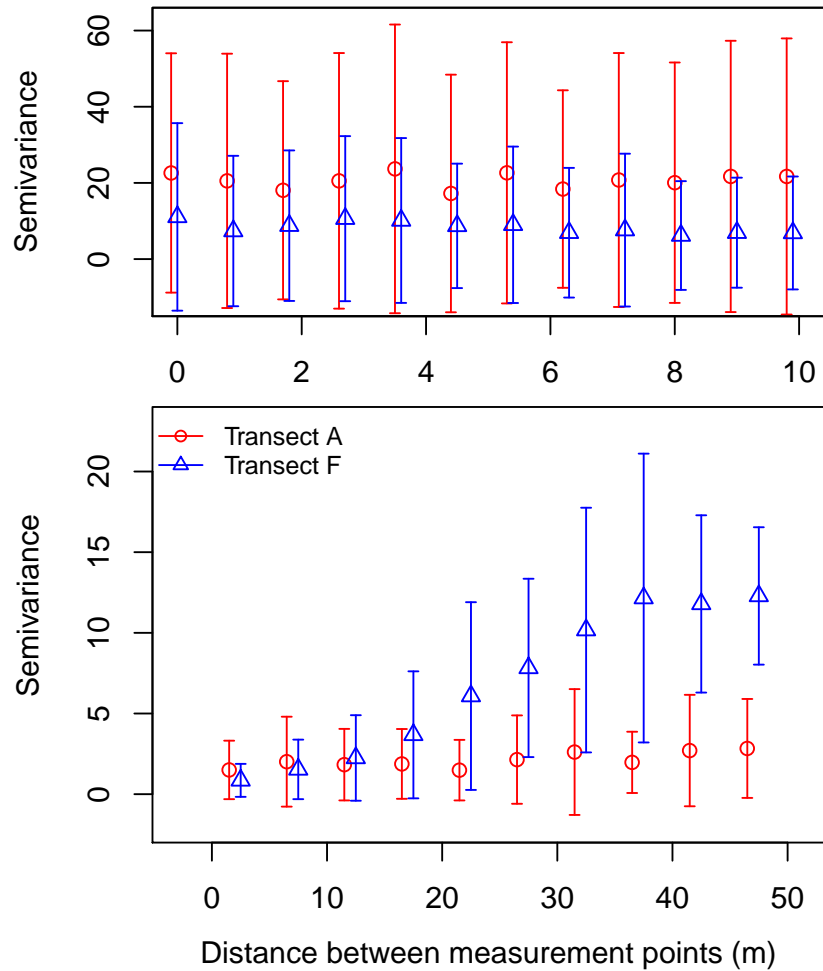


Figure 7: Semi-variogram for Transects A (red circles) and F (blue triangles) with  $\pm$  standard deviation as error bars. Upper panel: based on a single measurement day in Transect A and F of 101 randomly spaced intervals, with distances ranging from 1 cm to 2.8 m. A lack of spatial structure at scales smaller than 10 m is seen here. Lower panel: based on all volumetric soil moisture measurement points done during the observation period at a 2 m interval spacing in Transect A and F. The semivariance is seen to be lower here due to averaging out over all measurement days. A clear spatial structure is seen on the average soil moisture conditions for Transect F.

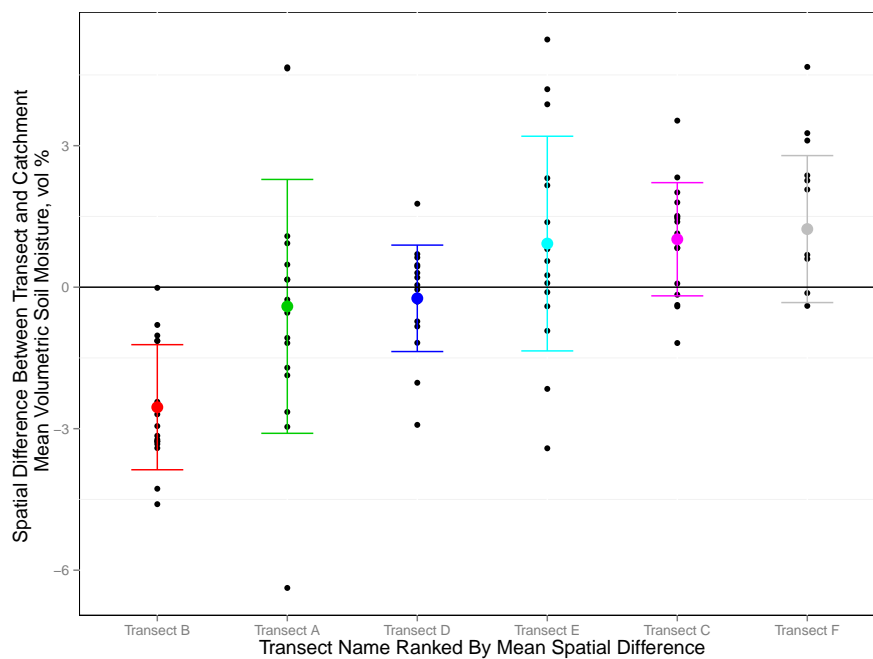


Figure 8: Rank stability plot for the different transect volumetric soil moisture means showing Transect D to be the most temporal stable transect. Black points indicate the spatial difference for each measurement day, the coloured points represent the mean over all measurement days. Error bars correspond to  $\pm 2$  times the standard deviation of the spatial differences.

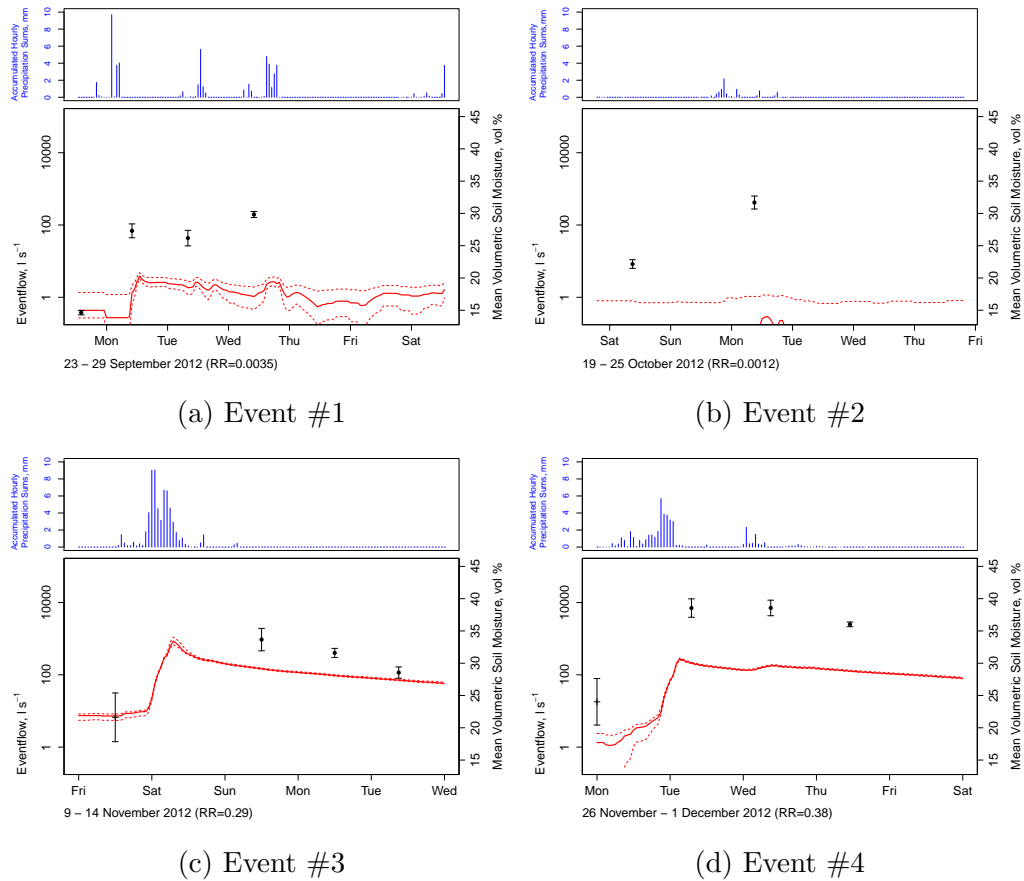


Figure 9: Influence of antecedent soil moisture conditions and precipitation on catchment response during four storm events are shown. Upper panels show hourly precipitation sums in mm as measured by an average of the two disdrometers located in the lower and upper part of the catchment. The lower panels display event flow (baseflow removed) plotted on a log scale as  $l s^{-1}$  as a solid red line. Dotted lines indicate the maximum and minimum limits of the discharge based on the error of the stage-discharge curve. The catchment mean volumetric soil moisture is shown in vol % as in situ data (filled circles) and ASCAT data (crosses). RR denotes the runoff ratio.

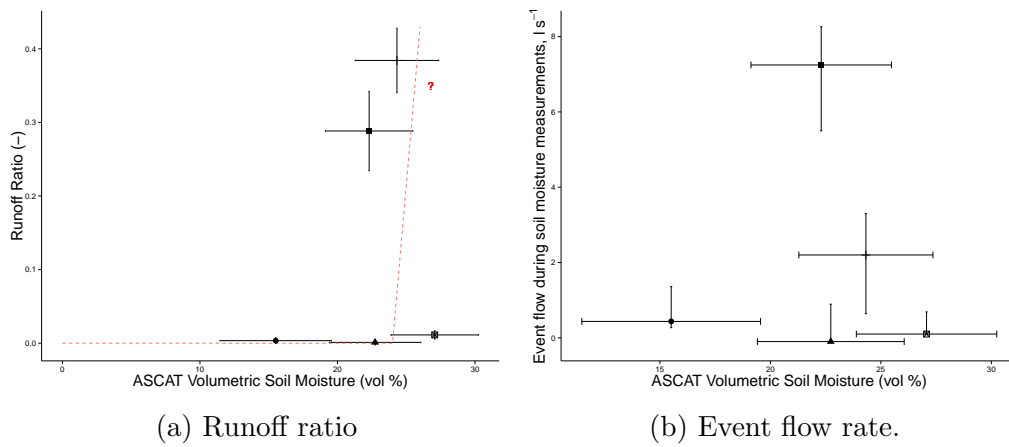


Figure 10: Relationship between runoff ratio (a) and event flow rate in  $l s^{-1}$  (b) with initial soil moisture content (source: ASCAT) for five precipitation events during the fall 2012. The different events are represented by the following symbols: diamonds (Event #1, 23-28 September), solid squares (Event #2, 19-22 October), triangles (Event #3, 9-17 November), no symbols (Event #4, 22 November-1 December), and hollow squares (Event #5, 23-31 October).